

On the Inclination Distribution of the Jovian Irregular Satellites

Valerio Carruba

Department of Astronomy, Cornell University, Ithaca, New York 14853
E-mail: valerio@astro.cornell.edu

Joseph A. Burns

Department of Astronomy and Department of Theoretical and Applied Mechanics, Cornell University, Ithaca, New York 14853

Philip D. Nicholson

Department of Astronomy, Cornell University, Ithaca, New York 14853

and

Brett J. Gladman

Observatoire de la Côte d'Azur, Nice, France 06304

Received February 13, 2002; revised April 17, 2002

Irregular satellites—moons that occupy large orbits of significant eccentricity e and/or inclination I —circle each of the giant planets. The irregulars often extend close to the orbital stability limit, about $1/3$ – $1/2$ of the way to the edge of their planet's Hill sphere. The distant, elongated, and inclined orbits suggest capture, which presumably would give a random distribution of inclinations. Yet, no known irregulars have inclinations (relative to the ecliptic) between 47° and 141° .

This paper shows that many high- I orbits are unstable due to secular solar perturbations. High-inclination orbits suffer appreciable periodic changes in eccentricity; large eccentricities can either drive particles with $\sim 70^\circ < I < 110^\circ$ deep into the realm of the regular satellites (where collisions and scatterings are likely to remove them from planetocentric orbits on a timescale of 10^7 – 10^9 years) or expel them from the Hill sphere of the planet.

By carrying out long-term (10^9 years) orbital integrations for a variety of hypothetical satellites, we demonstrate that solar and planetary perturbations, by causing particles to strike (or to escape) their planet, considerably broaden this zone of avoidance. It grows to at least $55^\circ < I < 130^\circ$ for orbits whose pericenters freely oscillate from 0 to 360° , while particles whose pericenters are locked at $\pm 90^\circ$ (Kozai mechanism) can remain for longer times.

We estimate that the stable phase space (over 10 Myr) for satellites trapped in the Kozai resonance contains $\sim 10\%$ of all stable orbits, suggesting the possible existence of a family of undiscovered objects at higher inclinations than those currently known.

© 2002 Elsevier Science (USA)

Key Words: satellites of Jupiter; celestial mechanics; orbits; origins.

I. INTRODUCTION

Using those few fragments remaining today, archaeologists reconstruct the birth and death of ancient civilizations. Planetary scientists may have a similar opportunity to decipher the origin of the giant planets by correctly interpreting the structure that is displayed in the orbital distributions of irregular satellites. Since the number of known irregular moons has nearly quadrupled to 39 in the past 4 years (see Gladman *et al.* 2001 and the references therein), we are now in a much better position to use their distinctive distributions to restrict possible origin scenarios.

The orbits of the irregular satellites (Fig. 1) have several notable characteristics. First, these moons are located at a few hundred planetary radii, an order of magnitude more distant from their planets than regular satellites (Burns 1986); this means that their paths fill significant fractions of their planets' Hill spheres. Second, orbits with inclinations I (measured relative to the planet's heliocentric orbital plane or, nearly equivalently, to the ecliptic) between $\sim 50^\circ$ and $\sim 140^\circ$ are not present, but otherwise orbit normals seem to be randomly oriented, filling about half of all solid angles. Lastly, the irregular satellites of the various planets are clustered in semimajor axis, inclination, and eccentricity, suggesting—as similarly inferred for asteroid families—one or more break-up events (Gladman *et al.* 2001).

Owing to their distant, highly eccentric, and substantially inclined orbits, the irregular satellites are generally believed to have once been independent planetesimals that were snared by the giant planets early in the Solar System's history (Burns 1986). When considered in the framework of the *circular*

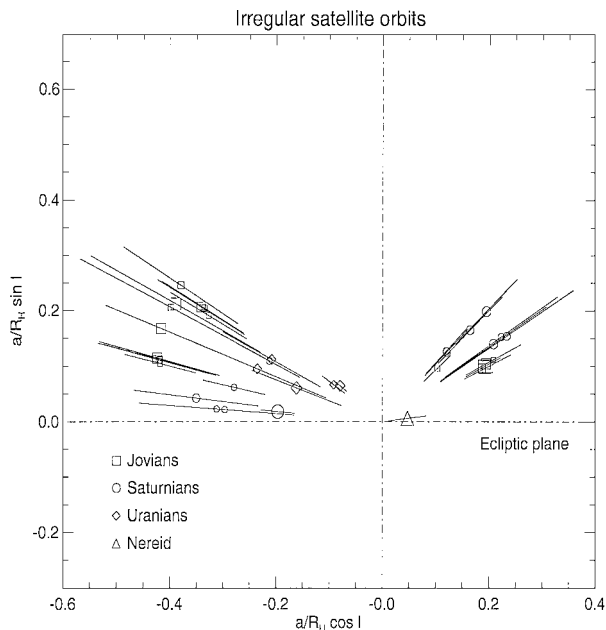


FIG. 1. The orbital properties of the known irregular satellites are displayed in this sketch; all the moons of any giant planet are represented by a distinct symbol. Each orbit's inclination I relative to the J2000 ecliptic (approximately the planet's orbital plane about the Sun) is depicted by the angle from the horizontal; moons in the right quadrant orbit in the same (direct) sense as their planets circle the Sun, while those in the left quadrant move retrograde (opposite to the planet's orbital motion). The radial distance from the origin to the symbol represents the orbit's semimajor axis a (given as a fraction of the radius of its planet's Hill sphere R_H ; see Eq. (1)). The length of each line illustrates the pericenter-to-apocenter variation in distance due to the orbital eccentricity e . A symbol's size is proportional to the logarithm of the satellite's radius, either measured or estimated from its magnitude and an assumed albedo of 6%. Time-averaged orbital elements (Jacobson 2001) are used to minimize the effect of solar perturbations. Reprinted by permission from *Nature*, Gladman *et al.*, **412**, 163–166, Copyright 2001, MacMillan Publishers Ltd.

restricted three-body problem (where a massless particle moves in the gravity field of the Sun, having mass m_\odot , and a giant planet of mass m moves in a circular orbit of radius r_\odot), a particle can be considered permanently captured only if it has sufficiently low energy so that its zero-velocity surface is closed. The *Jacobi constant* gives the particle's total energy in a reference frame that rotates with the mutual orbital motion of the primaries (Hamilton and Krivov 1997). The largest zero-velocity surface that encloses only m is called the *Hill sphere*; it has a mean radius

$$R_H = (\mu/3)^{1/3} r_\odot, \quad (1)$$

where $\mu = m/(m_\odot + m)$. Hamilton and Krivov (1997) argue analytically that particles will become unbound if they are started on uninclined, initially circular orbits at distances greater than $0.53 R_H$ (direct) and $0.69 R_H$ (retrograde). Hamilton and Burns (1992) maintain that the distance r_\odot should be replaced by the pericenter distance $q = a_\odot(1 - e_\odot)$ when the planet's orbit is rather eccentric.

Permanent capture from heliocentric orbit thus requires a change in the Jacobi constant. Two mechanisms have been proposed for the capture of irregular satellites. In the first, energy is lost while the particle is within the planet's Hill sphere, either through gas drag by a circumplanetary nebula (Pollack *et al.* 1979) or through collisions with comets or satellites (Colombo and Franklin 1971). In the alternative mechanism, rapid growth of the giant planet expands the zone of stable orbits (Heppenheimer and Porco 1977, Saha and Tremaine 1993) so that a particle, previously outside the Hill sphere, suddenly finds itself enveloped by a new, expanded Hill sphere.

II. THE SETTING

The orbital paths of the known irregular satellites are among the most complicated of any satellite paths in the Solar System (Kovalevsky and Sagnier 1977). The complexity of these motions has attracted both theoreticians and numerical analysts to investigate them, as Saha and Tremaine (1993) summarized. The already eccentric and inclined orbits are strongly disturbed by solar tugs. If a represents the satellite's orbital semimajor axis, a good measure of the solar perturbation's strength is $(a/R_H)^3$, which is between 0.064 and 0.097 for the retrograde jovian satellites. Excepting irregular satellites, Earth's Moon has the next largest solar perturbation of 0.018, only one-fourth as potent.

The histories of highly inclined orbits are distinct from those of nearly equatorial paths, as documented in various numerical simulations relevant to both Solar System problems (e.g., Hamilton and Burns 1991, Bailey *et al.* 1992, McKinnon *et al.* 1995) and hierarchical triple stellar systems, the latter most recently in connection with the extrasolar planet orbiting 16 Cygni B (e.g., Holman *et al.* 1997, Innanen *et al.* 1997, Mazeh *et al.* 1997). In such three-body systems, the tidal tugs of the distant body cause large coupled oscillations between the eccentricity and inclination of a small mass's orbit whose pericenter is free to range from 0 to 360° ("circulating orbits"). On the other hand, a particle whose pericenter oscillates ("librates") around 90° or 270° experiences more limited variations of eccentricity and inclination. This is referred to as the Kozai resonance.

As noted above, irregular satellites with mean orbital inclinations between 47° and 141° seem to be absent (Fig. 1). The remainder of this paper describes the circumstances under which solar perturbations, among others, cause the eccentricities of such bodies on circulating orbits to become large enough that either collisions ensue in the depths of the regular satellite system or the particles move so far from their planet that they are pulled by the Sun from planetocentric orbits. To understand how this may occur, and to estimate the relevant timescales, we first consider analytically the secular (time-averaged) effects of the Sun on orbits distant from a planet. Then we study numerically a more complete problem that includes the Sun's periodic nudges as well as those of the other giant planets. For simplicity, we restrict our detailed calculations to the jovian system.

III. SECULAR THEORY AND KOZAI OSCILLATIONS

To help interpret our numerical integrations, we start with the secular problem, following Innanen *et al.*'s. (1997) analysis. We choose a reference frame centered on Jupiter that revolves at that planet's heliocentric orbital rate; $\mathbf{r} = x\mathbf{i} + y\mathbf{j} + z\mathbf{k}$ is the particle's position with \mathbf{i} pointing away from the Sun and \mathbf{k} normal to Jupiter's orbit plane. Only the Sun's tidal potential affects the satellite's joviocentric orbit. Particles that are stationary in this reference frame experience a perturbation to their joviocentric orbits that pulls them along the solar direction away from Jupiter (proportional to $3x$) and into Jupiter's orbital plane (proportional to $-z$) (Hamilton and Burns 1991). In response to these forces, orbit planes precess and oscillate in eccentricity; *direct* (vs *retrograde*) orbits become most elongated when their lines of apsides align with (vs are at 90°) from the solar direction (Hamilton and Krivov 1997). At any position, the tidal potential R_I , to second and lowest order in r/r_\odot (which is a reasonable approximation, since in our case r/r_\odot is generally less than 0.001), is given by Kozai (1962).

$$R_I = G_0(m_\odot/r_\odot)(r/r_\odot)^2 P_2[\cos S], \quad (2)$$

where S is the angle between the position vectors \mathbf{r} and \mathbf{r}_\odot from Jupiter to the satellite and the Sun, respectively; P_2 is the second Legendre polynomial, and G_0 is the gravitational constant. Orbital periods for the irregular satellites range from about 6 months up to 7 years, whereas the giant planets circle the Sun in tens to hundreds of years. As we will learn below, the orbital shape and orientation oscillate over times measured in scores to thousands of years. Hence, if we are interested only in the orbit's long-term behavior, we can apply Gauss's approach in which the masses of the perturbing Sun and the satellite are smeared out along their paths with densities that are proportional to the times spent at the various places. This amounts to averaging (2) over the mean anomalies of the Sun and the satellite. The resulting secular tidal potential R_1 , also called the secular disturbing function, is

$$R_1 = G_0 m_\odot a^2 [2 + 3e^2 - (3 + 12e^2 - 15e^2 \cos^2 \omega) \sin^2 I] / (8b_\odot^3), \quad (3)$$

where a is the orbit's semimajor axis, ω is the argument of pericenter, and $b_\odot = a_\odot(1 - e_\odot^2)^{1/2}$ is the semiminor axis of Jupiter's orbit (Innanen *et al.* 1997). R_1 depends on Jupiter's eccentricity e_\odot only through the semiminor axis b_\odot . So we are effectively treating a case of the circular restricted three-body problem, in which the mass of the Sun is slightly increased. We can combine the osculating orbital elements ($a, e, I, \Omega, \omega, M$) (where Ω and M have the usual meaning of longitude of the nodes and mean anomaly) into the canonically conjugate Delaunay variables (Murray and Dermott 1999),

$$\begin{aligned} L &= \sqrt{\mu a}; & l &= M, \\ G &= \sqrt{\mu a(1 - e^2)}; & g &= \omega, \\ H &= \sqrt{\mu a(1 - e^2) \cos I}; & h &= \Omega, \end{aligned} \quad (4)$$

where $\mu = G_0(m_J)$ (m_J is the mass of Jupiter); $L = (\mu^2/2\varepsilon)^{1/2}$, with ε the specific (i.e., per unit mass) orbital energy, given by

$$\varepsilon = -G_0 m_J / 2a; \quad (5)$$

G is the specific orbital angular momentum; and H is the component of the specific orbital angular momentum that is perpendicular to Jupiter's orbit plane. In these variables, the secular disturbing function can be written as

$$R = \frac{-G_0 m_\odot L^4}{8b_\odot^3 \mu^2} \left[-10 + \frac{3}{L^2} (3G^2 - 4H^2) + 15 \frac{H^2}{G^2} + 15 \cos^2 g \left(1 - \frac{G^2}{L^2} - \frac{H^2}{G^2} + \frac{H^2}{L^2} \right) \right]. \quad (6)$$

Since this function does not depend on l , its conjugate variable L is a constant of the motion, which implies that the total specific orbital energy is also constant. Thus, under the action of tides, the satellite's orbit size does not change secularly. Similarly, since the disturbing function (6) does not involve h , its conjugate momentum H is conserved. Because both H and L remain constant, the behaviors of e and I must be coupled: as e reaches its minimum, $|\cos I|$ must also achieve its minimum. Keep in mind that these constancies, which result from the problem's symmetries, apply strictly only in the averaged problem where hoops of material replace the real bodies.

The secular evolution of the mean orbit can be found by using Hamilton's equations for the Delaunay variables and by transforming back into orbital elements. Alternatively, they can be derived from the planetary perturbation equations using (3) (Burns 1977, Murray and Dermott 1999). Either procedure yields

$$dI/d\tau = -(15/16)e^2(1 - e^2)^{-1/2} \sin 2\omega \sin 2I, \quad (7a)$$

$$de/d\tau = (15/8)e(1 - e^2)^{1/2} \sin 2\omega \sin^2 I, \quad (7b)$$

$$d\omega/d\tau = (3/4)(1 - e^2)^{1/2} \{2(1 - e^2) + 5 \sin^2 \omega [e^2 - \sin^2 I]\}, \quad (7c)$$

and

$$d\Omega/d\tau = -(\cos I/4)(1 - e^2)^{-1/2} [3 + 12e^2 - 15e^2 \cos 2\omega], \quad (7d)$$

where we have scaled time according to $t = (b_\odot^3 n / G_0 m_\odot) \tau$ (Innanen *et al.* 1997) with n the satellite's mean motion about its

planet. In principle, these nonlinear equations can be integrated, and their solutions can be expressed in terms of Jacobi elliptic functions (Kinoshita and Nakai 1991, 1999). In our work, we solve these equations numerically, by using a Runge–Kutta approach. Since all the dependent variables in (7) are dimensionless, the system’s evolution takes place over periods (Holman *et al.* 1997, Mazeh *et al.* 1997) of order

$$t_{sec} = 2\pi (b_{\odot}^3 n / G_0 m_{\odot}), \quad (8a)$$

or

$$\begin{aligned} t_{sec} &\sim P_{\text{orbit}}(m_J / m_{\odot})(a_{\odot}/a)^3 (1 - e_{\odot}^2)^{3/2} \\ &\sim 3P_{\text{orbit}} \times (R_H/a)^3 (1 - e_{\odot}^2)^{3/2}. \end{aligned} \quad (8b)$$

For nearly circular orbits of low inclination, the circulation period of ω is $2t_{sec}/3$, while the nodal regression period is $4t_{sec}/3$. For the actual jovian system, t_{sec} is about 180 years for most known prograde satellites and 65 years for the retrograde ones. An inspection of Eqs. (7) indicates that the amplitudes of the Kozai oscillations in e and I are independent of the distance to, and mass of, the perturbing Sun. As (8b) indicates, however, the timescale for these oscillations does vary with m_{\odot} and a_{\odot} .

The system’s evolution differs considerably according to whether the satellite *orbits lie close to Jupiter’s heliocentric orbit plane* or well out of it. For small e , the term within the curly brackets of (7c) is approximately $2 - 5 \sin^2 \omega \sin^2 I$; thus, $d\omega/d\tau$ will always be positive if $\sin^2 I < 2/5$ (i.e., when either $I < I_{crit} = 39.2^\circ$ or $I > I_{crit} = 140.8^\circ$). In these circumstances, ω will circulate, obliging the right-hand sides of (7a) and (7b) to oscillate. Thus the changes in e and I will alternate in sign; in addition, due to the factors e^2 and e , the right-hand sides of (7a) and (7b) will generally be small. Accordingly, the histories of e and I will be quasi-periodic, and the character of low-inclination orbits will scarcely change as ω circulates. A similar outcome will apply anytime ω drifts swiftly in one direction, for example, as a result of planetary oblateness acting on inner satellite orbits (Dermott and Nicholson 1986).

In contrast, for *paths that are highly inclined relative to Jupiter’s orbital plane*, i.e., those where $\sin^2 I > 2/5$, $d\omega/d\tau$ may change sign, meaning that ω can slow significantly or oscillate about $\pm\pi/2$. This allows e and I to vary substantially (see Eqs. (7a) and (7b), where $\sin \omega$ is now roughly constant).

R has only one degree of freedom, so trajectories in phase space track contours of R . Following the approach of Holman *et al.* (1997), we can describe the system in terms of the dimensionless momentum variable $x = 1 - e^2 = G^2/L^2$, the angle $\omega = g$, and the conserved quantity

$$\Theta = (1 - e^2) \cos^2 I = H^2/L^2.$$

In these variables, from Hamilton’s equations, $d\omega/dt$ (Eq. (7c)) is:

$$\frac{dg}{dt} = \frac{3G_0 m_{\odot} L^3}{4b_{\odot}^3 x^{3/2}} \left[3x^2 - 5\Theta + 5 \cos^2 g \left(\frac{3}{5} - x^2 \right) \right]. \quad (9)$$

For $\Theta < 3/5$ (which corresponds to $\sin^2 I > 2/5$ for $e_0 \ll 1$), a new class of solutions is possible, centered on the stationary point where $dg/dt = 0$ for $g = \pm 90^\circ$; i.e., $x = (5\Theta/3)^{1/2}$. Figure 2 shows the results of numerical integrations of Eqs. (7) for $\Theta = 0.25, 0.50$, and 0.7 in the phase space $x = 1 - e^2$ vs ω and I vs ω . Since this system is Hamiltonian, these trajectories can also be obtained by plotting equipotential levels of Eq. (6) (Kozai 1962, Holman *et al.* 1997). The presence of the libration island for $\Theta < 3/5$ is apparent. Figures 3 and 4 show the time evolution of e , I , and ω for orbits with $e_0 = 0.1$ and 0.4 , respectively. The reader may find it instructive to follow the associated curves in Fig. 2.

For $\Theta > 3/5$ (see Figs. 2a, b), ω circulates and we find the solutions previously described. Note that since Θ is conserved, trajectories cannot gain access to the region of phase space with $x \leq \Theta$ (or analogously, with $|\cos I| \geq \Theta^{1/2}$). The phase space available is therefore inversely related to the value of Θ . Variations in e and I are limited to a small range and ω increases monotonically (Figs. 3a and 4a).

For $\Theta \leq 3/5$ (see Figs. 2c, 2d, and 2e, 2f for $\Theta = 0.50$ and 0.25 , respectively), the phase space is now divided into regions in which the argument of perijove ω circulates, and zones in which ω librates about $\pm 90^\circ$. All solutions started with $\omega_0 = 0^\circ$ still circulate, only now the presence of a librating island forces the eccentricities to reach maxima when $\omega_0 = \pm 90^\circ$; thus e can be quite close to 1 for small values of Θ . For the same value of Θ , the maximum value of the eccentricity for circulating solutions is always greater than the maximum eccentricity of any librating solution. The constancy of Θ requires $(1 - e_0^2) \cos^2 I_0 = (1 - e_{max}^2) \cos^2 I_{min}$, where I_{min} is $\leq \sin^{-1}(2/5)^{1/2}$. Yet, as can be seen from Fig. 2 (or Fig. 5 below), the bottom of the libration island occurs at less than $I = 39.2^\circ$ (or $\cos I_{min} > 3/5$). For circulating solutions, it then follows that

$$e_{max} \geq [1 - 5 \cos^2 I_0/3]^{1/2} \quad (10)$$

for $e_0 \ll 1$. For example, for $\Theta = 0.25$ (Figs. 2e, f) and $I_0 = 60^\circ$ (or 120°), Eq. (10) predicts $e_{max} = 0.76$, or $x_{min} = 0.42$, for small e_0 . Figure 2e shows that in fact $x_{min} = 0.32$, or $e_{max} = 0.82$, so Eq. (10) is rather conservative. This is confirmed by Figs. 3b, 3d, 4b, and 4d. For smaller values of Θ , the libration island protrudes to smaller I , and consequently, the value of e_{max} at $\omega = \pm 90^\circ$ is bigger. Such large eccentricities may lead the body to penetrate the region of the regular satellites where close encounters can scatter it out of the system.

For $\omega_0 = \pm 90^\circ$, particles can now librate or circulate, depending on initial conditions. If the particle librates, changes in eccentricity are limited to a fixed range. It should, however, be pointed

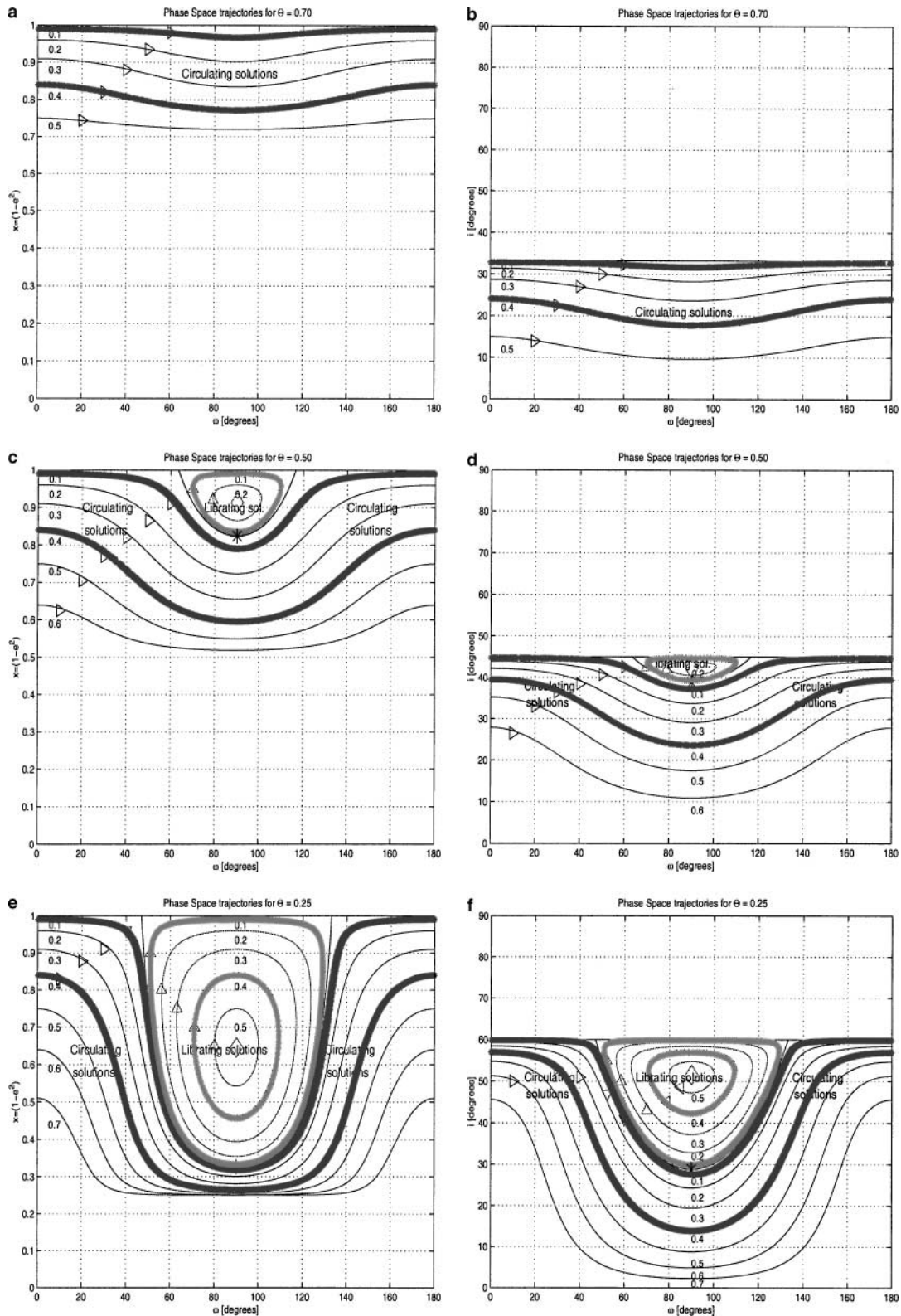


FIG. 2. Plots of $x = 1 - e^2$ vs ω and I vs ω derived from numerical solutions of Eqs. (7) for $\Theta = 0.70$ (Figs. a, b), 0.50 (Figs. c, d), 0.25 (Figs. e, f). Since the solutions are symmetrical around $\omega = 180^\circ$, we do not show the results for $\omega = 180^\circ \rightarrow 360^\circ$. Curves are labelled by the initial eccentricity (at $\omega = 0^\circ$ for circulating solutions, and at $\omega = 90^\circ$ for librating solutions). The diamonds in the middle of the libration zone locate the fixed points ($dg/dt = 0$ for $g = \pm 90^\circ$); the asterisks in Figs. c and f represent the minimum possible values of x (maximum of e) and I for librating solutions similar positions can be found in Figs. d and f. For $\Theta > 0.60$ (top panels), the libration island disappears and only circulating solutions are possible. The presence of the libration island for smaller values of Θ forces any circulating particle to reach larger values of maximum eccentricity when $\omega = 90^\circ$. The fixed points (e_F , I_F) are $(0.295, 42.26^\circ)$ for $\Theta = 0.50$ and $(0.595, 51.51^\circ)$ for $\Theta = 0.25$.

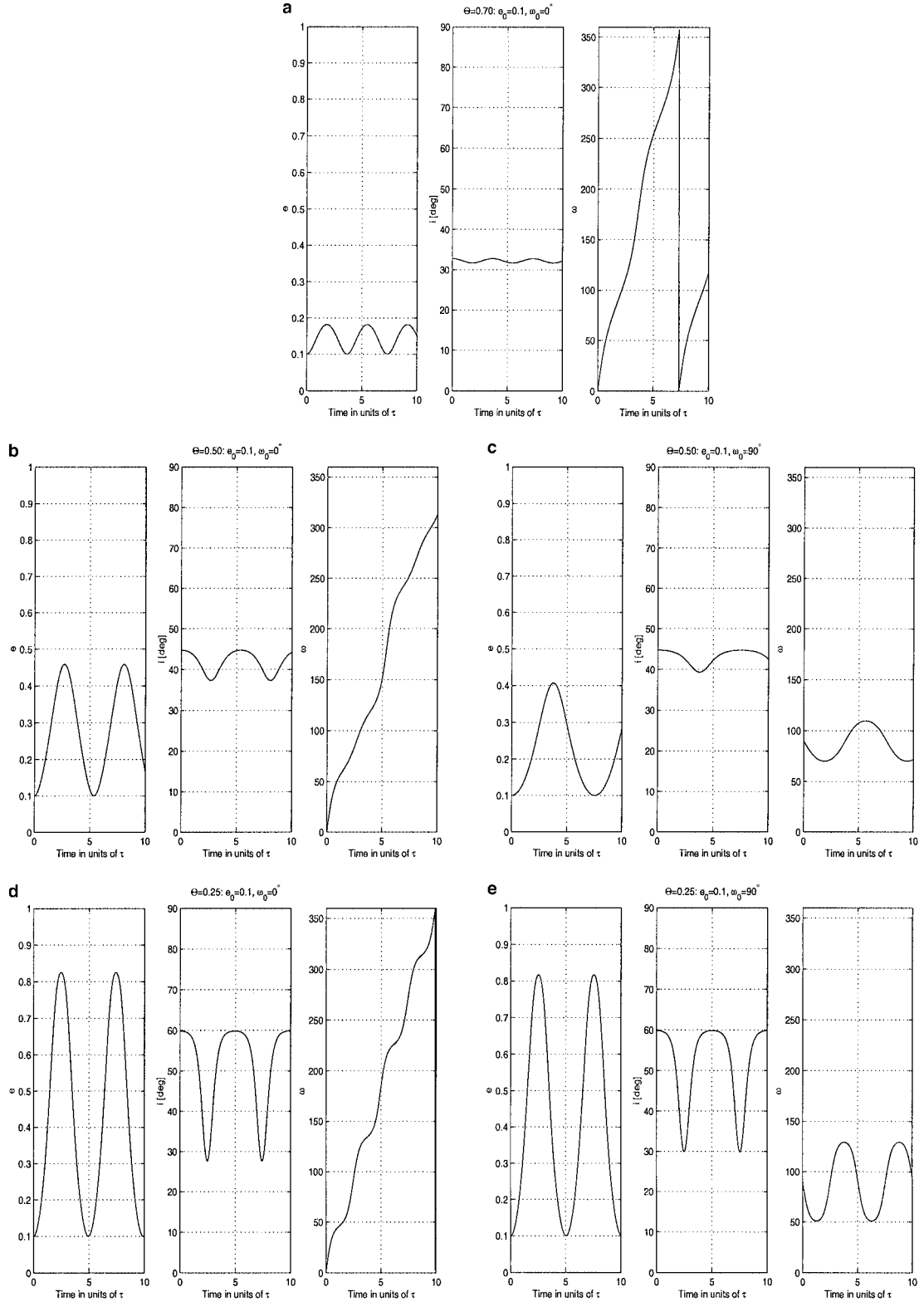


FIG. 3. Plots of e , i , and ω for $\Theta = 0.70$ (Fig. a) (where only circulating solutions are possible, and we choose $\omega_0 = 0^\circ$), and for $\Theta = 0.50$ (Figs. b and c) and 0.25 (Figs. d and e) (circulating ($\omega_0 = 0^\circ$) and librating solutions ($\omega_0 = 90^\circ$) for $e_0 = 0.1$). Since Θ is a conserved quantity, the maximum of the eccentricity corresponds to the minimum of the inclination and vice versa. For $\Theta > 0.6$, only circulating solutions are possible (ω goes from 0 to 360°) and variations in eccentricity and inclination cover a limited range. For $\Theta < 0.6$, both circulating and librating solutions are possible: due to the presence of the libration island, circulating solutions ($\omega_0 = 0^\circ$) experience a somewhat wider range of variation in e and i than do librating solutions ($\omega_0 = \pm 90^\circ$), which is smaller for orbits closer to the libration points, with larger initial eccentricity.

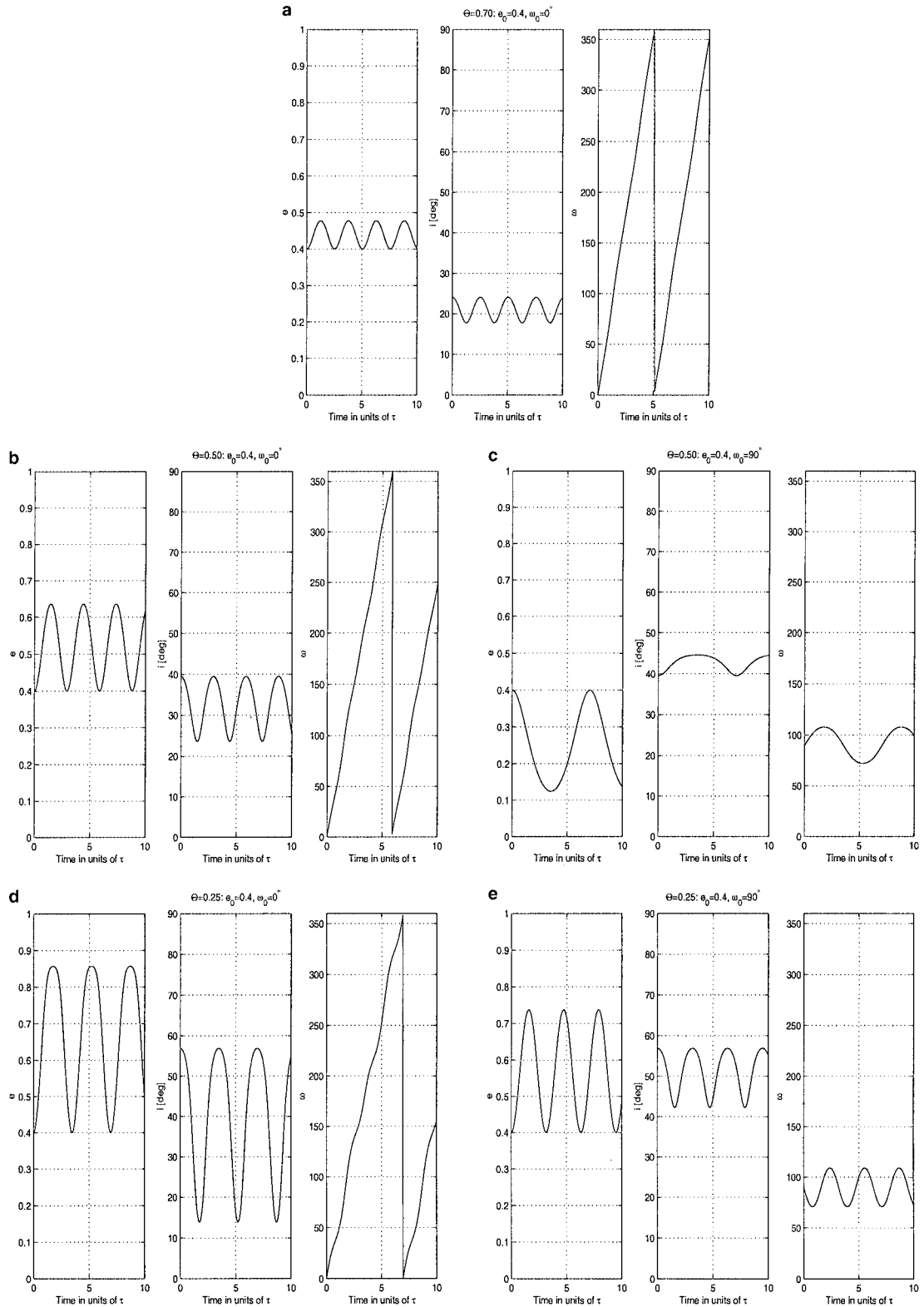


FIG. 4. Same as for Fig. 3, but for $e_0 = 0.4$. Note that the librating solutions are closer to the fixed points and thus have a more limited range of variations in e and I than those in Fig. 3.

out that this is rigorously true only within the assumptions of the averaged model. Numerical simulations by Holman *et al.* (1997) show that trajectories close to the separatrix are actually chaotic. Real trajectories near the separatrix may swap back and forth from circulation to libration. The period of libration is inversely proportional to the distance from the separatrix, closer orbits having longer libration periods. Figs. 3c, 3e, 4c, and 4e show that test particles on librating orbits whose initial conditions are closer to the fixed points, i.e., at larger eccentricities for smaller Θ , have a more restricted range of variation in e than the corresponding particles on circulating orbits. They can therefore be “protected” from having their pericenters brought into the region of the regular satellites.

We represent these histories in an alternative way in Fig. 5. For $a = 0.12$ AU, we show plots of constant Θ in the e - I plane. For $\Theta \geq 3/5$, only circulating solutions are possible (green lines). For $\Theta \leq 3/5$, librating and circulating solutions are both per-

mitted. The librating solutions must, however, lie within the libration island, so they range in eccentricity from 0 to a maximum value (black curve in the figure, determined numerically). These solutions are roughly symmetrical about the fixed points (red diamonds), which are located at

$$\cos I = \left(\frac{3\Theta}{5}\right)^{1/4}, \quad (11a)$$

and

$$e = \sqrt{1 - \left(\frac{5\Theta}{3}\right)^{1/2}}. \quad (11b)$$

They move with an amplitude that depends on the initial conditions (which is zero for particles started at the fixed point).

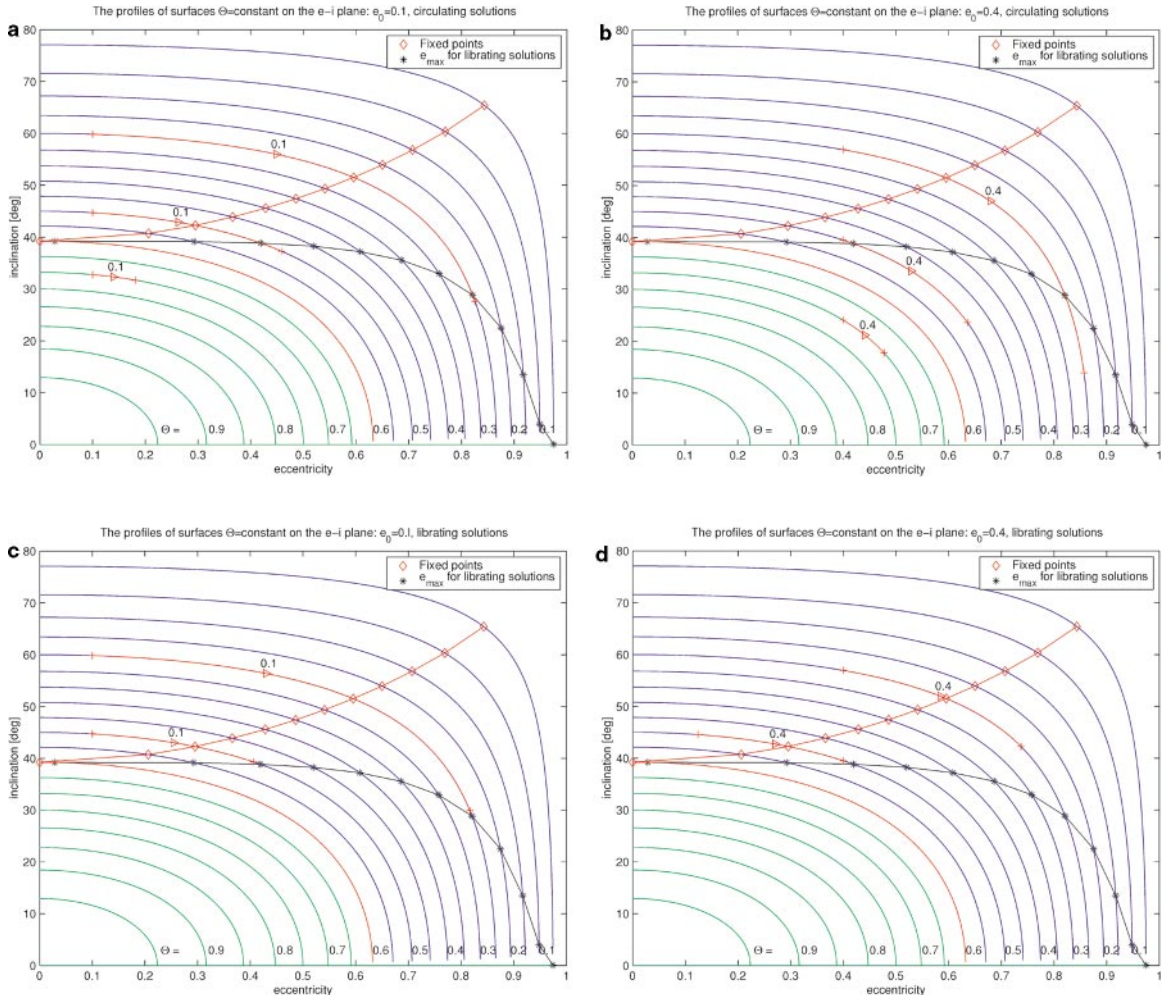


FIG. 5. Plots of $\Theta = \text{const.}$ In the e - I plane for $a = 0.12$ AU; numbers along the x -axis identify Θ values. The red curve for $\Theta = 0.6$ separates the region where librating solutions are possible from the region where they are not. The black line indicates the edge of the libration island, while the red line with diamonds connects the fixed points for different Θ . Superimposed on the lines of constant Θ we plot the range of variations in e and I for the orbits shown in Figs. 3 and 4. The first plot shows circulating solutions for $e_0 = 0.1$, the second circulating solutions for $e_0 = 0.4$, while the third and fourth give librating solutions for $e_0 = 0.1$ and $e_0 = 0.4$, respectively.

Superimposed on the lines of constant angular momentum, we plot the range of variations in e and I of the solutions shown in Figs. 3 and 4. Particles with $e_0 = 0.4$ and $\omega_0 = 90^\circ$ oscillate around the fixed point, so that the maximum value of their eccentricity is smaller than the corresponding value for circulating solutions.

The situation is more complicated if we consider the effects of perturbations from the other jovian planets or even if we address the nonaveraged problem with $e_J \neq 0$. Results of numerical simulations for this case are discussed in the following section.

IV. NUMERICAL SIMULATIONS OF SOLAR AND PLANETARY PERTURBATIONS ON INCLINED ORBITS

The explanation based on the Kozai oscillations given above partially accounts for the inclination distribution of the known irregular satellites. The model we developed in the previous section is, however, based on an approximate ($O(r^2/r_\odot^2)$) version of the disturbing function and does not include the effect of perturbations from the other jovian planets. To further explore the dynamics of the system, we performed numerical simulations that include the full perturbations of the Sun and incorporate the other giant planets.

Long-term numerical integrations for the jovian retrograde satellites have been carried out most recently by Whipple and Shelus (1993) for 10^5 years and by Saha and Tremaine (1993) for 2×10^6 years. Several earlier studies are referenced in these works and by Kovalevsky and Sagnier (1977). Saha and Tremaine (1993) used the fourth-order, mixed-variable symplectic algorithm of Wisdom and Holman (1991) with a typical step-size of 0.04 years. The integration included the Sun and the four giant planets, but not the terrestrial planets, Galilean satellites, Jupiter's oblateness, or relativistic effects.

Our first integrations to follow the orbital histories of the irregular satellites of Jupiter applied the WHM integrator of Wisdom and Holman (1991) as implemented in Duncan *et al.* (1998). Our time-step was 3.65 days, we integrated for 100 years, and oscillating elements were output every year. We accounted for the Sun (augmented by the masses of the terrestrial planets), Jupiter (with the Galilean satellite masses added), and the other giant planets; we do not include Jupiter's flattening nor relativistic effects. Our starting conditions were taken from the Jet Propulsion Laboratory (JPL) Horizons ephemeris.

A typical satellite history (Fig. 6), that of retrograde Pasiphae for a hundred years, shows fairly smooth drifts of ω and Ω with time ($\tilde{\omega}$ is defined as $\Omega - \omega$ for retrograde satellites). This full solution can be compared against the secular solution for similar circumstances, albeit for a prograde path (cf. Fig. 4a); the small wiggles for a in Fig. 6 correspond to tidal forcing as the satellite takes two years to orbit Jupiter, whose 12-year orbital period is readily visible. The periods ω and Ω take to precess fully are about 70 and 75 years, respectively, agreeing well with our secular prediction of 65 years from Eq. (8) and the 81 years

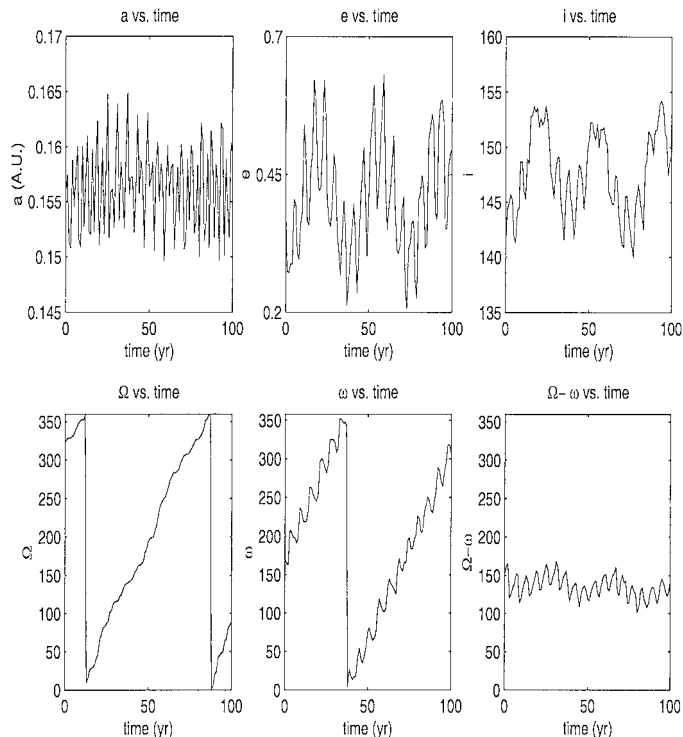


FIG. 6. The jovicentric orbit of retrograde Pasiphae, starting at J2000. The reference frame is the J2000 ecliptic and equinox. For a retrograde satellite, $\tilde{\omega}$ is defined as $\Omega - \omega$. The small wiggles in a , not present in the secular problem (Fig. 4a, prograde case), are due to tidal forcing. Note also the frequency associated with Jupiter's period (12 years).

listed on the JPL-SSD website. The long-term oscillations of e and I : (i) occur at about twice this frequency (like the tidal term itself), (ii) are substantial, and (iii) are *in-phase*, as expected for a retrograde satellite. Our results for the temporal character and amplitudes of this moon's orbital perturbations compare favorably to those of Whipple and Shelus (1993). By conducting a simulation over 300,000 years, we were able to replicate the results of Whipple and Shelus's (1993) identification of a secular resonance between Pasiphae's perijove e and Jupiter's perihelion. We have also checked that our numerical results for the classical jovian irregulars duplicate the integrations of Jacobson (2001) over the same interval (1000 years).

Figure 7 shows the results for integrations of test particles with the same initial conditions as those used for solving the secular problem (Fig. 4), with $e_0 = 0.4$ (results are analogous for $e_0 = 0.1$ and are not shown). The dominant features seen in Fig. 4—orbital precession at about t_{sec} associated with substantial oscillations in e and I —are quite evident. Now, in addition, high-frequency oscillations with periods of 6 years are visible; these result from the elliptical motions of the satellite and Jupiter that are, of course, not present in the secular problem (plus perturbations from the other jovian planets). Oscillations in e and I are still in antiphase, but Jupiter's orbit eccentricity and perturbations by the other jovian planets cause variations in

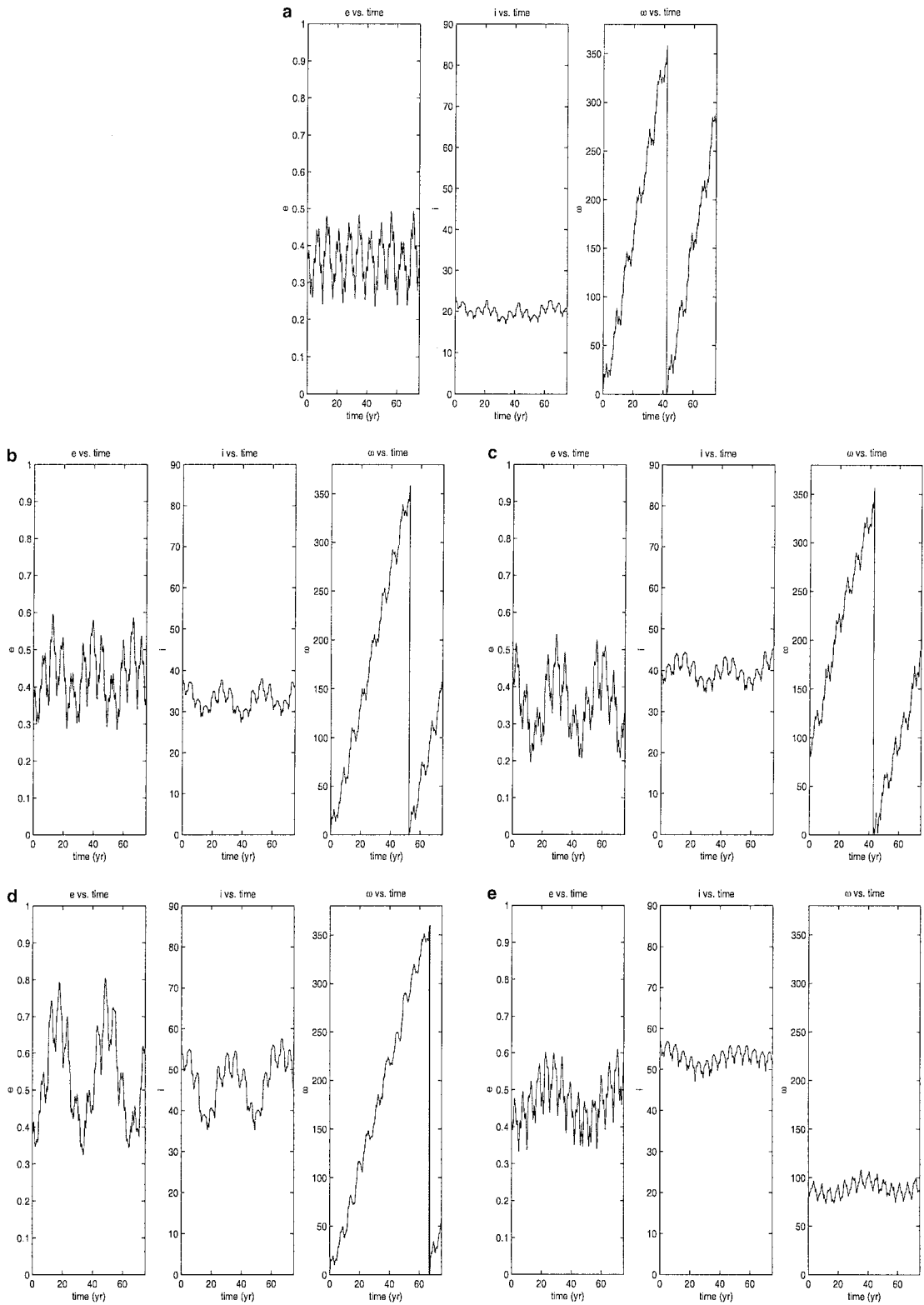


FIG. 7. Full numerical solution for the same problem whose secular solutions are plotted in Fig. 4. Osculating e , I , and ω histories are shown over 100 years for direct jovian satellites that start with $a_0 = 0.12$ AU and $e_0 = 0.4$. Note the oscillations in orbital elements with a period of 12 years, which are due to Jupiter's eccentric orbit. The particle with $\Theta = 0.5$ and $\omega_0 = 90^\circ$, which was librating in the secular problem (Fig. 4c), is now circulating. Figure a shows the circulating solution for $\Theta = 0.70$, Figs. b and c show the circulating and librating solutions for $\Theta = 0.50$, and Figs. d and e display the two cases for $\Theta = 0.25$.

the extrema for eccentricity and inclination, which now differ from cycle to cycle. The most striking difference from the secular problem is, however, for the particle in a librating orbit for $\Theta = 0.5$ (Fig. 4c), which, according to the results of the numerical simulation (Fig. 7c), is now circulating. As discussed in the previous section, particles close to the separatrix can be pushed by perturbations from the Sun or the other planets across that line and become circulating. Inspection of Fig. 5 shows that this librating solution was very near the maximum allowed value of e_0 . We will discuss this phenomenon in more detail while reporting other results of our long-term simulations.

Having tested our integrator against the previously determined histories of the tabulated irregular jovian satellites and guided by the results of our secular model, we considered the orbital evolution of an array of hypothetical objects over times as long as 10^9 years. The starting orbits of these bodies range in a from 0.08 AU to 0.20 AU, spaced at intervals of 0.02 AU. (Most known retrograde jovian satellites have semimajor axes slightly less than 0.16 AU, while the typical prograde satellite is at about 0.08 AU. For Jupiter, $R_H = 0.355$ AU). Our test particles had initial eccentricities e_0 of either 0.10 or 0.20 (the secular model predicts that the maximum eccentricity for circulating particles, reached at $\omega = \pm 90^\circ$, is not strongly dependent on e_0 , and is least for small values of e_0). Initial inclinations were in the range between 35 and 70° , and between 110 and 145° , separated by 5° (objects between 70 and 110° should have their pericenters forced into the region of the regular stellites, according to the secular theory (cf. Eq. (10)), so we do not consider them in our numerical simulations). This corresponds to values of Θ_0 (we use the initial value of Θ because for the problem with full perturbations from the Sun and the other jovian planets, Θ is no longer a conserved quantity) between 0.11 and 0.66 for $e_0 = 0.1$, and between 0.12 and 0.64 for $e_0 = 0.2$. Thus, we have investigated a total of (8 initial inclinations) \times (2 orbital directions) \times (7 semimajor axes) \times (2 initial eccentricities) = 224 cases. We took random values of Ω_0 , since this angle circulates with a typical period of ~ 80 years, and $\omega_0 = 0^\circ$, corresponding to circulating solutions (for these solutions, ω will cover the full range 0 – 360°). As discussed in the secular problem, for circulating particles the initial eccentricity is the minimum value, while the initial inclination is a maximum (minimum for retrograde particles).

We integrated these test particles over 10^9 years using a longer time-step—15 days—and plotted osculating orbital elements smoothed with a running window with a period of 1000 years and a shift of 100 years. Particles are considered to be lost once they penetrate a sphere having twice the planet's radius and to have escaped once their distance from Jupiter exceeds the radius of the Hill sphere (Eq. (1)). The end states of the individual particles are shown for $e_0 = 0.1$ (Fig. 8) and for $e_0 = 0.2$ (Figs. 9 and 10). These integrations indicate that many orbits are gradually lost due to the interaction of periodic and secular perturbations over longer time spans. Most lost particles escape to heliocentric orbits. As integrations were extended, particle orbits were more likely to become highly eccentric, paralleling

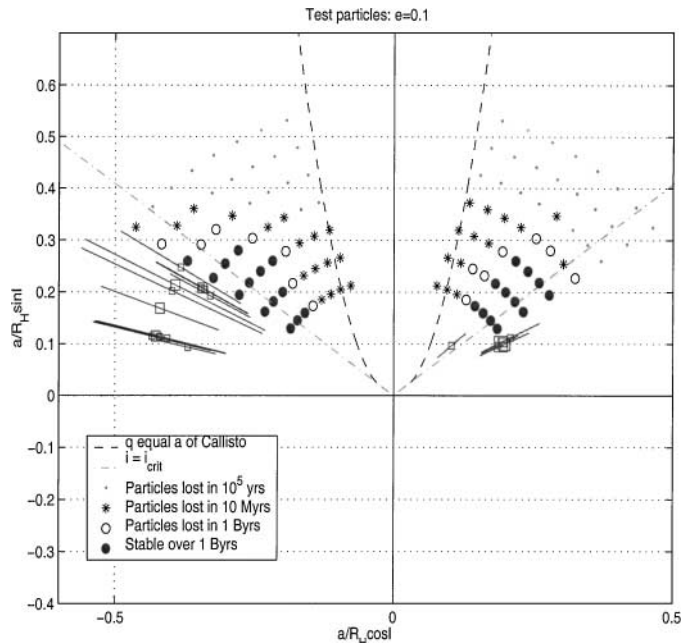


FIG. 8. The final fate of 112 jovian test particles with $e_0 = 0.1$ and $\omega_0 = 0^\circ$. The orbits of the known jovian satellites are shown as lines with squares (cf. Fig. 1). The dashed straight lines separate high- I behaviors from low- I ones in the secular problem, while the dashed parabola encloses the zone of avoidance according to Eq. (10). Dots correspond to objects that escaped from Jupiter in 10^5 years; asterisks took between 10^5 and 10^7 years to die; open circles were lost in less than 1 Byr. Filled circles indicate particles that remained stable over more than a Byr.

results for asteroidal orbits near the many resonances that permeate the main belt (Wisdom 1983, Morbidelli and Nesvorný 1999, Murray *et al.* 1998). Thus the zone of instability grows as orbital integration times increase, and with our longest integrations (10^9 years), we observe that almost all the (a, I) space where irregular satellites are missing turns out to be unstable. We anticipate that even longer integrations ($t \rightarrow 4.5 \times 10^9$ years) would disclose that many of the remaining niches for circulating satellites lose stability as well. (The word stability is intended in the sense of effective stability, as described in Giorgilli and Skokos 1997 and Skokos and Dokoumetzidis 2001).

Other satellites may be destabilized by interactions with the Galilean satellites. Gravitational assists during fly-bys of Galileans can easily boost orbital energies sufficiently to release these objects from Jupiter's gravitational grasp (when at high eccentricities, the retrograde irregular satellites have typical orbital velocities relative to Jupiter at aphelia that are only a few hundred m/s. Thus, a relatively small disturbance at the nodes of the Galilean satellites' orbits can dislodge previously trapped objects). Gravity assists by the Galilean satellites approach the surface escape velocity or 1–2 km/sec. Figure 10 displays the pericenter evolution of a particle that eventually collides with Jupiter. This particle pierced deeply into the realm of Galilean satellites (whose semimajor axes are shown in the plot) and could have easily experienced a close encounter, or even a collision,

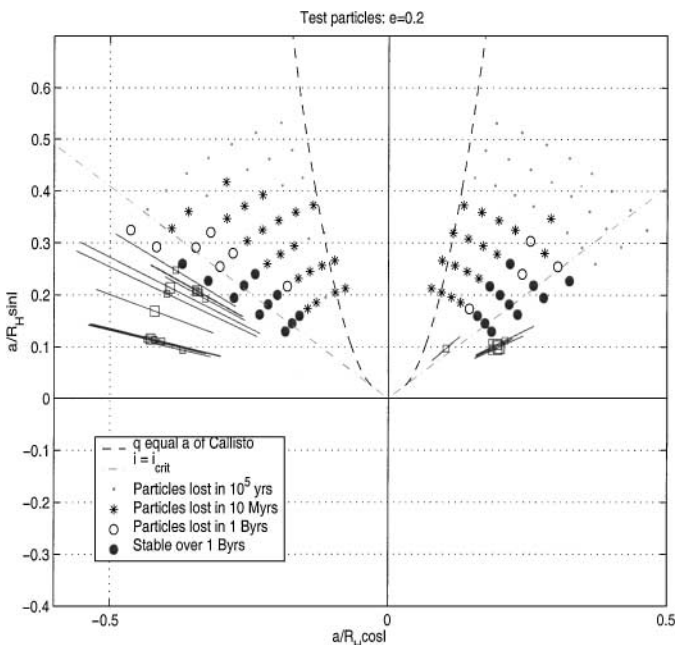


FIG. 9. The final fate of 112 jovian test particles with $e_0 = 0.2$ and $\omega_0 = 0^\circ$. The orbits of the known jovian satellites are shown as lines with squares (cf. Fig. 1). The dashed straight lines separate high- I behaviors from low- I ones in the secular problem, while the dashed parabola gives the zone of avoidance according to Eq. (10). Dots correspond to objects that escaped from Jupiter in 10^5 years; asterisks took between 10^5 and 10^7 years to die; open circles were lost in less than 1 Byr. Filled circles indicate particles that remained stable over more than a Byr.

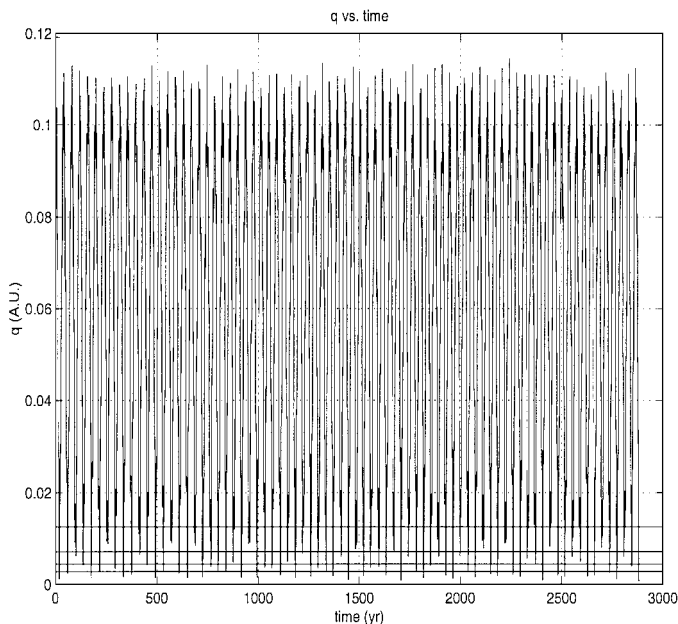


FIG. 10. Pericenter distance for a particle started with $a_0 = 0.14$ AU, $e_0 = 0.2$, and $I_0 = 110^\circ$. The semimajor axes of the Galilean satellites are the horizontal lines at the bottom of the plot. This particle hit Jupiter at 2840 years.

if it passed by the nodes of its orbits with those of the regular satellites at the right time.

We notice that particles are stripped away once their initial orbits extend out to a significant fraction of the Hill sphere, in agreement with the original numerical results of Hénon (1970). It also appears, in accordance with the same paper and with Hamilton and Burns (1991) and Hamilton and Krivov (1997), that objects on retrograde orbits are somewhat more stable than prograde ones at the same semimajor axis. A similar dichotomy is visible among the extant jovian satellites but is not apparent within Saturn's retinue (Gladman *et al.* 2001). Even though our grid is fairly coarse, we believe that our simulations provide a meaningful survey of the stability of the outer regions of the Hill sphere. Saha and Tremaine (1993) have determined that orbits in this vicinity are chaotic with Lyapunov timescales of about 5000 years. Thus, it is not surprising to see that the outcomes of our simulations are not uniform, with occasional islands of relative stability.

To investigate whether stable librating solutions might exist in the complete problem, we started particles with initial conditions that lie within the libration island of the secular problem ($\omega_0 = 90^\circ$ and $\Theta_0 < 0.6$). As discussed in the previous section, $\Theta_0 = (1 - e_0^2) \cos^2 I_0$ is a conserved quantity in the secular problem. For our simulations, we choose particles with the same value of Θ_0 and increasing values of eccentricity ($e = 0.1$ – 0.9 , when possible). Figure 11 shows on e – I plots lines of constant Θ_0 containing our grid of initial conditions. We also plot a line showing orbits whose pericenter is closer to Jupiter than Callisto. This does not necessarily mean that those particles can experience a close encounter with that satellite, since in order to do that they need to be at the nodes of their orbits with Callisto's at the same time as the Galilean satellite. We found that this was, however, a useful first-order criterion to distinguish orbits that actually can be gravitationally scattered from those that cannot. Particles whose initial conditions are in the upper region of librating orbits can also interact with Callisto; all these are most likely to be lost on short timescales. We carried out integrations across a grid of 73 particles in e and I , for five different distances from Jupiter— $a = 0.06, 0.09, 0.12, 0.15,$ and 0.18 AU—for both prograde and retrograde particles. Results of our integrations for three cases (prograde and retrograde particles, and results of an integration over 100 Myr for $a = 0.12$ AU) are shown in Fig. 11. Particles at $a = 0.18$ AU were all lost in less than 3000 years.

Due to short-period perturbations from the Sun and the other jovian planets, orbits that were librating in the secular problem can escape from the libration island and begin circulating, as indicated by stars in Fig. 11. Because fully perturbed orbits are not obliged to follow the results of the secular model very closely, in Fig. 12 we report the result of a numerical simulation for $\Theta = 0.25$ and $e_0 = 0.4$ ($a = 0.12$ AU), superimposed on the secular solutions of Eqs. (7) for the same initial conditions (cf. Figs. 4e and 7e). The orbit jumps back and forth in the neighborhood of the secular solution but remains bounded by the separatrix (i.e., the particle stays trapped in the Kozai resonance).

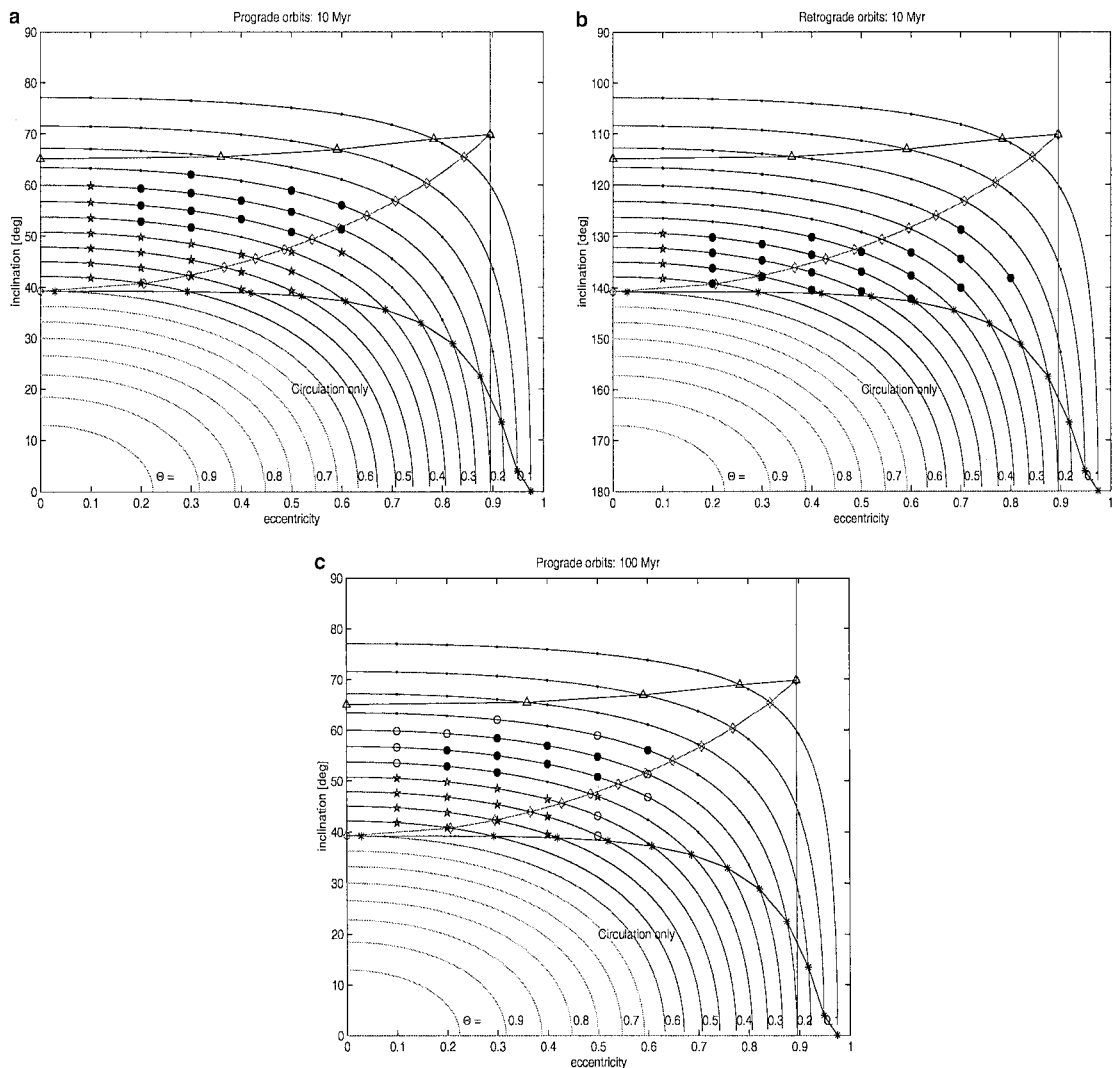


FIG. 11. Lines of constant angular momentum $\Theta = (1 - e^2) \cos^2 I$ in the e - I plane for $a = 0.12$ AU, both prograde and retrograde cases (first and second panels, respectively). The lower line with asterisks represents the lower limit of the libration island; particles with initial e and I below that line can only circulate, while above both circulating and librating solutions are possible. The line with diamonds locates the libration points, while the vertical line on the right indicates the eccentricity needed by particles at that distance from Jupiter to have its q equal to Callisto's a . Of course, particles whose initial conditions are in the upper region of librating orbits that can interact with Callisto are most likely going to be lost on short timescales. We indicate the boundary for such orbits with a black line with triangles. We report the fate of 73 particles for each value of a (for both the prograde and retrograde cases). Filled circles are particles that were stable over 10 Myr; small black dots are particles that were lost (either they escaped from the Hill sphere of Jupiter or they crashed into the planet); and stars are particles not bound to the libration island (they crossed the separatrix during the course of the integration and became circulating particles). For $a = 0.12$ AU, prograde case, we extended the simulation to 100 Myr (third panel); open circles are particles lost over this longer timescale. This longer simulation and previous results for circulating particles suggest that at least some particles not locked into the libration island should be unstable over timescales longer than 10 Myr.

Particles whose initial conditions approach the separatrix can eventually leave the libration island.

Librating particles are most stable for values of e_0 and I_0 close to those of the fixed points. Prograde particles with a value of Θ_0 near 0.6, the limiting value for the existence of librating solutions, are not confined to the libration island, and as can be inferred from the results of previous simulations on circulating particles, they are probably lost over longer timescales (10^9 years). This seems to be confirmed by an integration for $a = 0.12$ AU over 100 Myr in which several of the particles that

were circulating in a previous integration of 10 Myr escaped or crashed into Jupiter. Results are similar for particles started in the second libration island at $\omega = 270^\circ$. Prograde librating particles are stable for large values of I , and strangely enough, the fates of particles with the same Θ_0 , above and below the fixed point, are not the same. Retrograde particles with $\Theta_0 \leq 0.3$ at $a = 0.09$ and 0.12 AU are all unstable within 10 Myr, while this is not the case for prograde particles. Some of the retrograde particles are stable for very large values of e (>0.7), and particles symmetric around the fixed point tend to share the same fate.

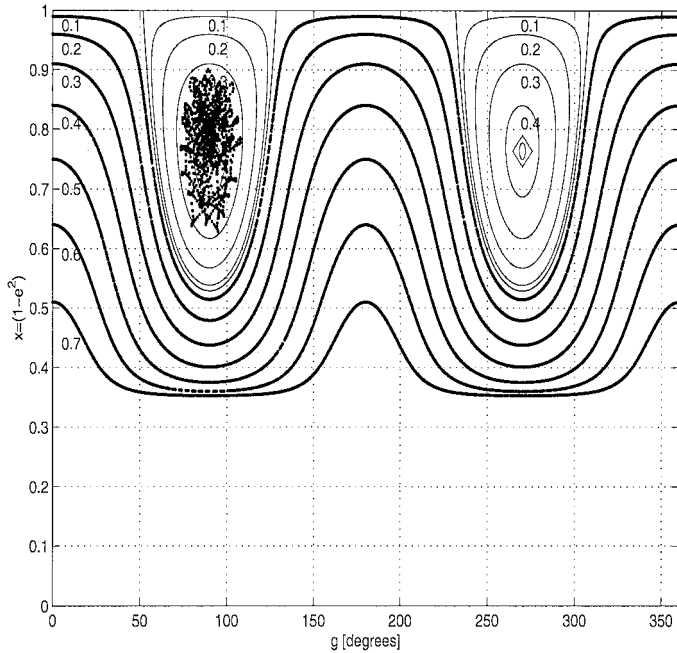


FIG. 12. The result of a numerical simulation for $\Theta_0 = 0.25$ and $e_0 = 0.4$ ($a = 0.12$ AU) over 100 yrs, with a sampling time of 30 days, superimposed on the phase plane solutions of Eqs. (7) for the same initial conditions.

Moreover, particles with values of Θ_0 close to 0.6 do not circulate for the retrograde case: the shape of the libration island for the case in which perturbations from the jovian planets are considered seems to be no longer symmetrical, as was the case for the averaged three-body model.

Figure 13 presents the results of simulations in the a - I plane ($e = 0.1, 0.3,$ and 0.5). These figures are analogous to Figs. 8 and 9 used to show results of circulating particles. In contrast to the case of circulating particles, librating particles with larger values of ($e_0 \cong 0.5$), which have initial conditions closer to the libration point, tend to be more stable than the analogous particles with lower eccentricity. Also, in contrast to the circulating case, prograde particles tend to be stable for larger values of initial inclination than the analogous retrograde ones. Although our simulations cover only a limited interval of time (10 Myr), we think they give valuable hints about the actual shape of the phase space region where librating particles can be stable. The results of the longer simulation seem to indicate that particles with the smaller values of Θ_0 (0.20–0.25 for the prograde case, 0.25–0.35 for the retrograde case) are lost on longer timescales, which roughly translates into a loss of objects at higher inclinations. While this paper was under revision, we became aware of an analogous study by D. N. Nesvorný *et al.* (personal communication, 2002). In their work, Nesvorný *et al.* integrated 8281 test orbits around Jupiter for the circulating ($\omega_0 = 0^\circ$) and librating ($\omega_0 = 0^\circ$) cases, with random values of Ω and M and values of e_0 of 0, 0.25, 0.5, and 0.75, over 0.5 Myr. In agreement with what we found in this work, Nesvorný *et al.*'s results show

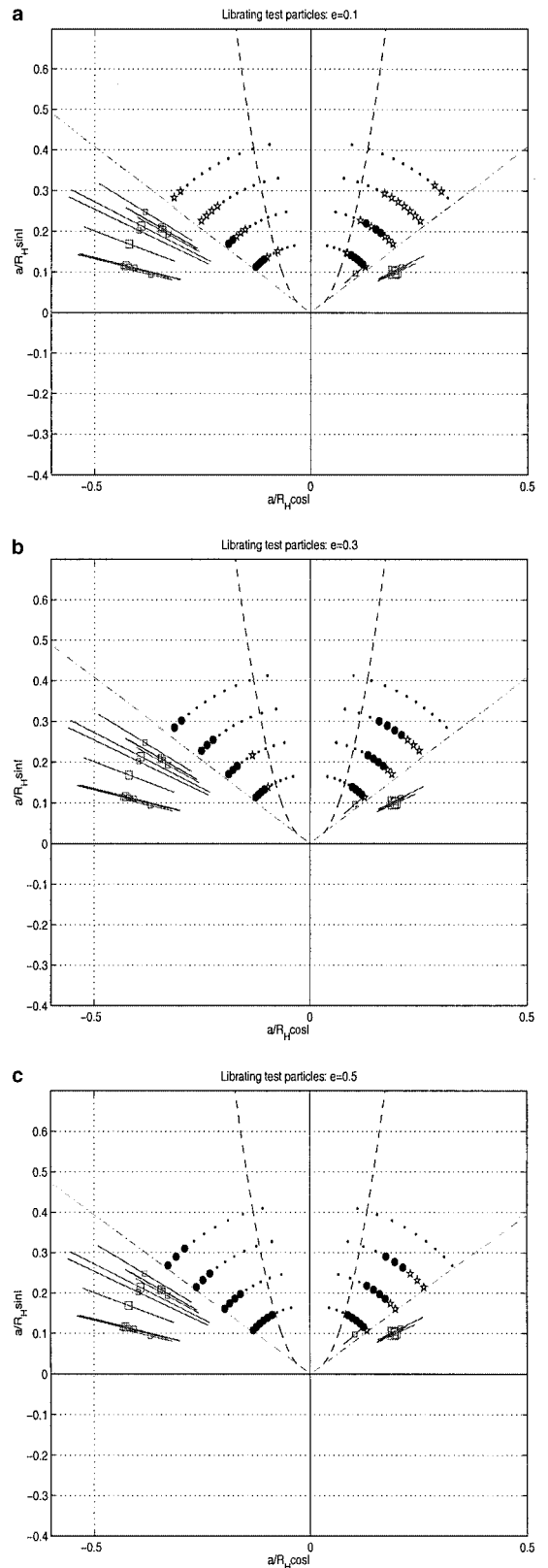


FIG. 13. The final fate of librating particles with $e_0 = 0.1, 0.3,$ and 0.5 . Lines and symbols have the same meaning as in Fig. 9. Stars represent particles not bound to the libration island.

that librating particles with high values of eccentricity (0.5 or 0.75) can be stable for values of i_0 up to 65–70°.

V. LIBRATING SATELLITES: ESTIMATES ON THEIR POPULATION

Since our simulations suggest that irregular satellites in the prograde and retrograde libration islands can be stable for at least 10 Myr, we now estimate the number of possible satellites in that region, assuming that all available phase space was uniformly populated initially. To achieve this goal, we need to estimate three quantities:

1. The fraction of the libration island over which orbits are stable = f_1 .
2. The portion of phase space for $\Theta < 0.6$ occupied by the libration island = f_2 .
3. The ratio between the phase space where libration islands are possible ($\Theta < 0.6$) and the phase space where only circulating orbits are allowed = f_3 .

We can approximate the first quantity from our simulations that provide the number of stable particles in the libration island compared to the total number of particles (73) for each value of the semimajor axis that we studied ($a = 0.06, 0.09, 0.12,$ and 0.15 AU). In this region, 26% ($=f_1$) of the test particles were stable over the 10-Myr integrations. We then computed the fraction of phase space covered by the libration island ($\Theta < 0.6$) by determining the fraction of the (g, G) phase space occupied by the libration island for different values of $H(=(\mu a \Theta)^{1/2})$. Since $G = (\mu a(1 - e^2))^{1/2} = (\mu a x)^{1/2}$, this fraction would be given by:

$$f_2 = \frac{\sum_i [4(90^\circ - g(i))\Delta x(i)^{1/2}]}{360^\circ(1 - \Theta^{1/2})}, \quad (12)$$

where g is computed from 0 to 90°, $\Delta x^{1/2}$ is the corresponding interval in $x^{1/2}$ (the factor 4 accounts for the other half of the libration island and for the other libration island at $\omega = 270^\circ$). The available phase space goes from $\Theta^{1/2}$ to 1, since H is conserved. This result is independent of the semimajor axis. Figure 14 plots the fraction f_2 of phase space occupied by the libration island as a function of $H/(\mu a)^{1/2}$; the average value of f_2 for that interval was 7%. Finally, we have to compute f_3 : we have seen that the total phase space available is given by:

$$V_{\text{phase space}} = 360^\circ \sqrt{(\mu a)}(1 - \sqrt{\Theta}). \quad (13)$$

After integrating Eq. (13) over the range of Θ for which librating solutions are possible (0.0–0.6) and for the values that allow only circulating solutions (0.6–0.1), we take the ratio of the results to determine that f_3 equals 6.72, independent of a . Assuming that all the circulating phase space is stable, and that circulating solutions are not stable in the librating region (which is rather pessimistic, since our simulations with circulating par-

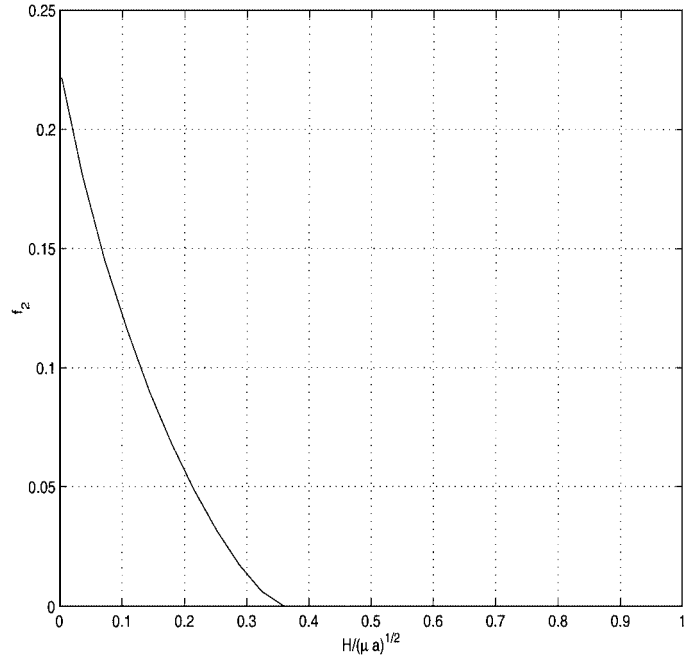


FIG. 14. The fraction of phase space occupied by the libration island as a function of $H/(\mu a)^{1/2}$.

ticles show that a region of stability exists for $\Theta \leq 0.6$), then the fraction of stable librating orbits compared to the stable circulating solutions is given by

$$f_4 = f_1 f_2 f_3 = 0.122;$$

that is, the libration islands occupy 12.2% of the phase space available to circulating solutions. Therefore, with the assumption that circulating solutions in the librating region are not stable, stable librating orbits occupy $12.2/(12.2 + 100) = 10.8\%$ of the available stable phase space. We assume that the available stable phase space was uniformly populated (which may be far from the truth, since it is dependent on the capture mechanism: gas drag, for example, should preferentially capture particles with small eccentricity ($e < 0.2$); this would exclude most of the stable librating satellites we found in our simulations that had $e > 0.3$). Thus, we would expect to find approximately 10% of the satellites in librating orbits at high inclinations. Since only one-quarter of Jupiter's Hill's sphere has been searched so far (B. Gladman, private communication, 2001), if we assume a total number of jovian irregular moons larger than 1 km in diameter of ~ 100 , this would suggest that there can be up to 10 objects in librating orbits that await discovery.

VI. CONCLUSIONS

We have described how the distinctive inclination distribution of the known irregular satellites may result from various dynamical processes. In particular, we have shown that, considering

just secular solar perturbations, highly inclined orbits ($70^\circ < I < 110^\circ$; i.e., those nearly normal to the planet's heliocentric orbit) are unlikely to be long-lived. The eccentricities of such orbits become large, periodically plunging the particles down to regions where collisions with the planet or gravitational scattering by regular satellites can occur. Rather, and more frequently, particles on such orbits are pulled away from the Hill sphere of the planet due to solar perturbations. We then demonstrated, through 10^9 -years numerical integrations of hypothetical irregular objects about Jupiter, that planetary and solar perturbations substantially widen this region (to $\sim 55^\circ < I < \sim 130^\circ$) for circulating particles.

On the other hand, some satellites librating in the Kozai resonance can be stable for 10 Myr or more. They have higher values of inclinations than those on stable circulating orbits. We estimate that $\sim 10\%$ of the irregular satellites of Jupiter could be Kozai resonators, if the capture process uniformly populated the phase space around the planet.

ACKNOWLEDGMENTS

We have benefited from sage advice by Hal Levison, David Nesvorný, Matija Cuk, Doug Hamilton, Alessandro Morbidelli, Charalampos Skokos, and Luke Dones about integration algorithms and the orbital histories of irregulars. We also thank the two referees, Hiroshi Kinoshita and Giovanni Gronchi, for useful comments and suggestions.

Note added in proof: Since the submission of this paper 11 new satellites of Jupiter have been discovered (MPEC J54).

REFERENCES

- Bailey, M. E., J. E. Chambers, and G. Hahn 1992. Origin of sungrazers: A frequent cometary end-state. *Astron. Astrophys.* **257**, 315–322.
- Burns, J. A. 1977. An elementary derivation of the perturbation equations of celestial mechanics. *Am. J. Phys.* **44**, 944–949; *Erratum* **45**, 1230.
- Burns, J. A. 1986. Some background on satellites. In *Satellites* (J. A. Burns and M. S. Matthews, Eds.), pp. 1–38. Univ. of Arizona Press, Tucson.
- Colombo, G., and F. A. Franklin 1971. On the formation of the outer satellite groups of Jupiter. *Icarus* **15**, 186–189.
- Cuk, M., and J. Burns 2001. Gas-assisted capture of the irregular satellites of Jupiter. *Bull. Am. Astron. Soc.* **33**, 1085 (abstract).
- Dermott, S. F., and P. D. Nicholson 1986. Masses of the satellites of Uranus. *Nature* **319**, 115–120.
- Duncan, M. J., H. F. Levison, and M. H. Lee 1998. A multiple time-step symplectic algorithm for integrating close encounters. *Astron. J.* **116**, 2067–2077.
- Giorgilli, A., and C. Skokos 1997. On the stability of the Trojan asteroids. *Astron. Astrophys.* **317**, 254–261.
- Gladman, B., J. J. Kavelaars, M. Holman, P. D. Nicholson, J. A. Burns, C. Hergenrother, J.-M. Petit, B. G. Marsden, R. Jacobson, W. Gray, and T. Grav 2001. Orbital clustering for twelve newly discovered Saturnian satellites: Evidence for collisional families. *Nature* **412**, 163–166.
- Hamilton, D. P., and J. A. Burns 1991. Orbital stability zones about asteroids. *Icarus* **92**, 118–131.
- Hamilton, D. P., and J. A. Burns 1992. Orbital stability zones about asteroids. II. The destabilizing effects of eccentric orbits and of solar radiation. *Icarus* **96**, 43–64.
- Hamilton, D. P., and A. V. Krivov 1997. Dynamics of distant moons of asteroids. *Icarus* **128**, 241–249.
- Hénon, M. 1970. Numerical exploration of the restricted problem. VI. Hill's case: Non-periodic orbits. *Astron. Astrophys.* **9**, 24–36.
- Heppenheimer, T. A., and C. C. Porco 1977. New contributions to the problem of capture. *Icarus* **30**, 385–401.
- Holman, M., J. Touma, and S. Tremaine 1997. Chaotic variations in the eccentricity of the planet orbiting 16 Cygni B. *Nature* **386**, 254–256.
- Innanen, K. A., J. Q. Zheng, S. Mikkola, and M. J. Valtonen 1997. The Kozai mechanism and the stability of planetary orbits in binary star systems. *Astron. J.* **113**, 1915–1919.
- Jacobson, R. A. 2001. The orbits of the recently discovered jovian and saturnian satellites. *BAAS* **33**, 1191.
- Kessler, D. J. 1981. Derivation of the collision probability between orbiting objects: The lifetimes of Jupiter's outer moons. *Icarus* **48**, 39–48.
- Kinoshita, H., and H. Nakai 1991. Secular perturbations of fictitious satellites of Uranus. *Celest. Mech. Dynam. Astron.* **52**, 293–303.
- Kinoshita, H., and H. Nakai 1999. Analytical solution of the Kozai resonance and its application. *Celest. Mech. Dynam. Astron.* **75**, 125–147.
- Kovalevsky, J., and J.-L. Sagnier 1977. The motions of satellites. In *Planetary Satellites* (J. A. Burns, Ed.), pp. 43–62. Univ. of Arizona Press, Tucson.
- Kowal, C. T., K. Aksnes, B. G. Marsden, and E. Roemer 1975. The thirteenth satellite of Jupiter. *Astron. J.* **80**, 460–464.
- Kozai, Y. 1962. Secular perturbations of asteroids with high inclination and eccentricity. *Astron. J.* **67**, 591–598.
- Mazeh, T., Y. Krymolowski, and G. Rosenfeld 1997. The high eccentricity of the planet orbiting 16 Cygni B. *Astrophys. J.* **477**, L103–106.
- McKinnon, W. B., J. I. Lunine, and D. Banfield 1995. Origin and evolution of Triton. In *Neptune and Triton* (D. P. Cruikshank, Ed.), pp. 807–878. Univ. of Arizona Press, Tucson.
- Morbidelli, A., and D. Nesvorný 1999. Numerous weak resonances drive asteroids toward terrestrial planets' orbits. *Icarus* **139**, 295–308.
- Murray, C. D., and S. F. Dermott 1999. *Solar System Dynamics*. Cambridge Univ. Press, Cambridge, UK.
- Murray, N., M. Holman, and M. Potter 1998. On the origin of chaos in the Solar System. *Astron. J.* **116**, 2583–2589.
- Pollack, J. B., J. A. Burns, and M. E. Tauber 1979. Gas drag in primordial circumplanetary envelopes: A mechanism for satellite capture. *Icarus* **37**, 587–611.
- Saha, P., and S. Tremaine 1993. The orbits of the retrograde jovian satellites. *Icarus* **106**, 549–562.
- Skokos, C., and A. Dokoumetzidis 2001. Effective stability of the Trojan asteroids. *Astron. Astrophys.* **367**, 729–736.
- Thomas, F., and A. Morbidelli 1996. On the Kozai resonance in the outer Solar System and the evolution of long-period comets. *Celest. Mech. Dynam. Astron.* **64**, 209–229.
- Weigert, P., K. Innanen, and S. Mikkola 2000. The stability of quasi-satellites in the outer Solar System. *Astron. J.* **119**, 1978–1984.
- Whipple, A., and P. J. Shelus 1993. A secular resonance between Jupiter and its eighth satellite? *Icarus* **101**, 265–271.
- Wisdom, J. 1983. Chaotic behavior and the origin of the 3/1 Kirkwood gap. *Icarus* **56**, 51–74.
- Wisdom, J., and M. J. Holman 1991. Symplectic maps for the n-body problem. *Astron. J.* **102**, 1528–1538.
- Zahnle, K., L. Dones, and H. F. Levison 1998. Cratering rates on the Galilean satellites. *Icarus* **136**, 202–222.